Key Points:
- Persistent neutral density and temperature enhancements are observed within 30 min of the dusk terminator
- A persistent neutral density enhancement is also observed prior to the dawn terminator at around 4–5 local time
- The neutral density features are observed in all species and appear to be associated with enhancements in neutral temperature

Correspondence to:
M. Pilinski,
marcin.pilinski@lasp.colorado.edu

First Evidence of Persistent Nighttime Temperature Structures in the Neutral Thermosphere of Mars

M. Pilinski[1] (iD), **S. Bougher[2]** (iD), **K. Greer[1]** (iD), **E. Thiemann[1]** (iD), **L. Andersson[1]** (iD), **M. Benna[3]** (iD), and **M. Elrod[3,4]** (iD)

[1]LASP, University of Colorado Boulder, Boulder, CO, USA, [2]Climate and Space Sciences and Engineering (CLASP), University of Michigan, Ann Arbor, MI, USA, [3]NASA Goddard Spaceflight Center, Greenbelt, MD, USA, [4]CRESST, University of Maryland College Park, College Park, MD, USA

Abstract Using two Mars years of data collected by the Neutral Gas and Ion Mass Spectrometer on the Mars Atmosphere and Volatiles EvolutioN spacecraft, we reconstruct the local solar time structure of the Martian equatorial thermosphere for the dawn and dusk sectors. The results indicate the presence of several persistent features near the dusk and dawn terminators appearing in the neutral temperature and in the O, Ar, N_2, and CO_2 densities. The dusk temperature features include a minimum at the terminator surrounded by two local maxima with amplitudes between 20 and 40 K. A nighttime temperature enhancement occurs at a local solar time of 4–5 hr and has an amplitude between 50 and 100 K relative to the surrounding temperatures. The observed enhancements are interpreted to be a result of either nighttime dynamical heating caused by converging and downwelling winds or of a terminator wave originating in the lower atmosphere.

Plain Language Summary NASA's Mars Atmosphere and Volatiles EvolutioN (MAVEN) spacecraft has been collecting information about the Mars' upper atmosphere since November 2014. In our study we examined the temperature in the upper atmosphere measured by a gas analyzer on MAVEN that periodically *sniffs* the air around it. By combining several years of data, we reconstructed a map of atmospheric temperatures dividing it into equatorial daytime, morning, evening, and nighttime regions. The results indicate that local patches of warm atmosphere extend about 300–600 km along the Martian equator (3–6 hr driving distance at highway speeds) on the nightside near morning and evening. One possible reason for these nighttime warm spots is the air currents in the Martian upper atmosphere. As the sun heats the dayside atmosphere, it expands and causes wind currents to blow away from the dayside region. These wind currents can extend away from the equator then return on the nightside colliding in the morning and evening regions. The resulting meeting of wind currents can heat the upper atmosphere. Warmer air escapes from the upper atmosphere faster. Because of this, these nighttime patches of warm air could have contributed to a faster escape of Martian atmospheric gases than previously believed.

1. Introduction

Thermospheric density features that are fixed relative to local solar time (LST; stationary features) serve as important indicators of the dynamics and global circulation that lead to their formation. Where these features are persistent (lasting through many seasons and solar conditions), they can also have a significant effect on the coupling with other regions of the atmosphere affecting, among other things, the sources of atmospheric escape. Stationary structures also contribute significantly to the aerodynamic drag experienced by satellites as their periapses drift through local time and latitude and can therefore fly through such features repeatedly over the course of many orbits or days. In this paper, we provide the first observational evidence for stationary density enhancements associated with dynamical forcing near the dawn and dusk terminators in the Martian thermosphere.

Large day-night density and temperature gradients in the Martian thermosphere lead to significant thermospheric winds. These winds form a global circulation pattern which is responsible for the redistribution of atmospheric mass and energy across the planet (Bougher, Brain, et al., 2017). Where these winds diverge (resulting in upwelling), the thermosphere can be adiabatically cooled decreasing the temperature from radiative equilibrium and therefore attenuating the neutral densities at a fixed altitude. Conversely, where

strong thermospheric winds converge and subside (resulting in downwelling), the atmosphere can be locally heated causing densities at fixed altitude levels to increase. Numerical model studies of the Martian thermosphere indicate that the global circulation at Mars should give rise to a nighttime enhancement in temperature and density above 150 km as a result of dynamical heating caused by converging winds (Bougher et al., 1990; Bougher, Pawlowski, et al., 2015; Gonzalez-Galindo et al., 2010; Nicholson, 2011). This nighttime *heat island* was first identified in a global circulation model by Bougher et al. (1990) as a large temperature feature that exists in the equatorial thermosphere at equinox. Morning enhancements located westward of the dawn terminator near the equator are also predicted by equinox models (Bougher, Pawlowski, et al., 2015).

Recent observations made by the Mars Atmosphere and Volatiles EvolutioN (MAVEN) spacecraft Neutral Gas and Ion Mass Spectrometer (NGIMS) enable the investigation of stationary features manifested in neutral thermospheric densities and temperatures at altitudes above 150 km. In this paper, we analyze the meridionally averaged neutral composition data collected by MAVEN using 20-min local time bins across a variety of species and during various seasons and extreme ultraviolet (EUV) forcing conditions. This analysis suggests that persistent maxima and minima in neutral densities occur near the Martian terminators.

Section 2 provides a description of the data. The details of the data processing are presented in section 3. The results showing the stationary thermospheric features and their properties are described in section 4.

2. Data

The MAVEN spacecraft began science operations at Mars in October 2014. It is nominally in an elliptical, $150 \times 6,000$ km, orbit with a 4.5-hr period and an inclination of 75° with respect to the Martian equator. An in-depth review of MAVEN and its mission is provided by Jakosky et al. (2015). In this work, we analyze the NGIMS data collected between February 2015 and November 2017. The NGIMS data set is described in detail by Mahaffy et al. (2014). In this analysis, we use the closed source neutral mode (Mahaffy et al., 2014). While NGIMS measures composition on both ascending and descending phases of its orbit, the post-periapsis outgassing of nonvolatile gases (O and CO_2) from the instrument walls dominate the measured signal during ascending passes making them unsuitable for our analysis. Argon densities are not significantly affected by this phenomenon enabling the use of data from both ascending and descending phases. NGIMS data are available on the Planetary Data System in the NGIMS Level-2 closed source data products, version 7, revision 3. All data used for this analysis are available on the Planetary Data System site and the process for development of the level 2 product is described in the NGIMS Software Interface Specification.

EUV irradiance is used to describe the amount of solar forcing incident upon the Martian dayside thermosphere when neutral densities are being observed. The MAVEN EUV Monitor measures the variability of solar soft X-rays and EUV irradiance at Mars. It consists of three broadband radiometers including the 121–122 nm filter (Lyman-α). In this work, we use the orbit average Lyman-_x237A; contained in the Level-2, version 11, revision 1, data product (Eparvier et al., 2015).

Due to the inclination of the orbit, MAVEN samples the equatorial thermosphere below 300 km altitude along a section of its trajectory that extends through ~1–2 hr of local time and ~40° latitude when the periapsis location is near the equator. In addition to the orbital motion, seasonal changes in the location of the MAVEN periapsis cause the equatorial thermospheric coverage to migrate to lower latitudes at a rate of approximately 30° latitude (aerographic) per month and to lower local times at a rate of approximately 3 hr per month.

3. Methods

The measured quantities analyzed in this work are Ar, N_2, CO_2, and O neutral number densities. Statistical distributions of measured quantities are organized into LST, latitude, and altitude bins. Data binning is performed according to the Mars-Sun-Orbit (MSO) reference frame to minimize the effects of solar declination along the Mars orbit. The MSO frame x axis points toward the sun and the z axis is aligned with the Mars-orbit normal vector. Locations in this frame are expressed as MSO Latitude and LST_{MSO} where LST_{MSO} is the MSO longitude converted to a 24-hr basis such that 0° MSO latitude and 12 LST_{MSO} correspond to the subsolar point, and 6 and 18 LST_{MSO} correspond with the dawn and dusk terminators, respectively.

The data presented here are restricted to low MSO latitudes for reasons related to latitudinal coverage of MAVEN periapsis sampling. Due to the in situ sampling of the thermospheric region between 150 and 220 km by MAVEN's elliptical orbit, there are variations in latitudinal coverage along different local times. In order to avoid aliasing changes resulting from latitudinal coverage and midlatitude/high-latitude features not associated with thermospheric features in question, the data analysis will be restricted to ±35° MSO latitudes. The local time data coverage across this *low* latitude band is relatively consistent and data in this band cover most local times for a variety of altitudes.

The statistical distribution of measurements within each bin is tracked for all measured quantities during the binning process. Each measurement is added to the overall distribution in a specific LST_{MSO}-latitude-altitude bin. Once the distributions have been collected in each bin, the overall mean and variance at that location can be computed. In this analysis, each density bin spans 20 min in LST (approximately 300 km horizontal distance) and 10 km in altitude.

A comparison with modeled temperatures from the Mars Global Ionosphere-Thermosphere Model (M-GITM) is provided in this paper. M-GITM is a model framework essentially combining the terrestrial GITM framework (e.g., Ridley et al., 2006) with Mars fundamental physical parameters, ion-neutral chemistry, and key radiative processes in order to capture the basic observed features of the thermal, compositional, and dynamical structure of the Mars atmosphere from the ground to ~250 km (e.g., Bougher, Pawlowski, et al., 2015). Unlike the Earth GITM code, the new M-GITM code currently simulates the conditions of the Martian atmosphere all the way to the surface. A suite of M-GITM simulations has been compared with MAVEN measurements obtained during its first 2 years of operations. This includes sampling during six Deep Dip campaigns (e.g., Bougher, Bell, et al., 2015; Bougher, Jakosky, et al., 2015; Zurek et al., 2017) as well as dayside science orbits (e.g., Bougher, Brain, et al., 2017; Bougher, Roeten, et al., 2017). MAVEN NGIMS, Imaging Ultraviolet Spectrograph, and Accelerometer measurements have been used to validate the M-GITM code.

Neutral temperatures are computed by integrating the hydrostatic equilibrium equation along the Argon density-altitude profiles using a method described by Snowden et al. (2013). Argon is used in order to take advantage of data from both ascending and descending passes (see next section). The temperature bins used in this analysis are equivalent in local time and latitude to the density bins but are 30 km tall in altitude in order to improve the statistics. Temperatures centered on 200 km altitude ($T_{N,200km}$), close to the Martian exobase, will be used because the altitude variability of temperature at this height is not expected to be large under the hydrostatic equilibrium assumption. The uncertainty of the temperature retrieval at 200 km altitude is expected to be 5–10 K. This uncertainty was estimated by repeatedly applying the temperature retrieval algorithm to M-GITM density profiles (N_2 and CO_2) which had random errors added (1-sigma normal distribution) corresponding to twice the NGIMS density uncertainty reported in the L-2 data product. This Monte Carlo analysis was performed at each local time in the equatorial region and the resulting 5–10 K range of errors corresponds to the spatial variation of the temperature uncertainty at 200 km altitude. A temperature retrieval bias of 0–8 K was also estimated by computing the mean difference between each Monte Carlo retrieval and the M-GITM temperature field. The temperature bias is less relevant to this work as we primarily focus on the relative changes in temperature along the horizontal direction. Furthermore, the Argon measurement signal-to-noise ratio is also sufficient for analysis at this altitude. Atmospheric waves result in 20–50% variability around the hydrostatic mean and require that multiple passes must be combined to recover the average thermospheric behavior.

4. Results

Examples of CO_2 density-altitude profiles (not binned) from descending (inbound) passes in September of 2016 are shown in Figure 1 (dotted lines). The MAVEN periapsis was near the MSO equator, while Mars was near perihelion during this time. As seen in Figure 1, activity in the Martian upper atmosphere (see, e.g., England et al., 2017 and references within) results in altitude profiles that change significantly from orbit to orbit (compare dotted lines of the same color). A median value of CO_2 density profiles grouped by local time is indicated in Figure 1 by solid lines. These median density profiles reflect the background state of the thermosphere as it is driven by solar activity and features of the thermospheric global circulation pattern during the time of the measurement. MAVEN's orbital precession causes the local time near periapsis to
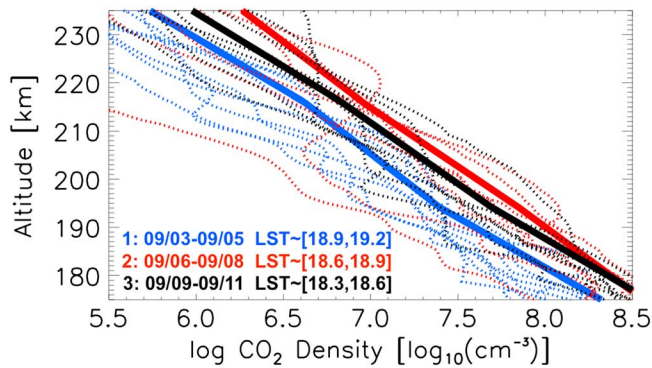
Figure 1. Three groups of descending pass neutral densities measured in 2016 and organized by approximate local time near 180 km. Dotted lines indicate individual passes while the thick lines are the median profiles of each set. Local time progression is 19–19.3 (blue) to 18.7–19 LST (red), and finally 18.4 to 18.7 LST (black). Note the enhanced densities between 18.7 and 19 LST (red) compared to the surrounding local times. LST = local solar time.

decrease. Thus, when the satellite flying near 180 km altitude, the mean local-time (MSO) of the observations varies from approximately 19.2 to 18.9 LST_{MSO} as indicated in the legend. One might expect the neutral density to increase monotonically between nighttime and the dusk terminator. However, Figure 1 indicates that as the local time decreases toward the dusk terminator, the mean density increases between 18 and 19 LST_{MSO} before decreasing closer to the dusk terminator.

It is not yet clear from Figure 1 whether this increase in density between 19 and 20 LST_{MSO} is caused by heating enhancements, changes in latitude, or an increase in EUV corresponding to the time when the spacecraft sampled this local time region. Due to the large variability in densities from orbit to orbit as well as the large-scale of the features we seek to identify, these data are best interpreted through a statistical analysis that organizes the data into local time and EUV bins in a single band of latitudes.

Figure 2 shows the binned neutral densities as a function of MSO local time and for an altitude of 180 km observed during 2016 (near perihelion, southern hemisphere summer). Each bin spans 20 min in LST and contains ~10 MAVEN orbits with NGIMS data. Figure 2a shows the CO_2, O, N_2, and Ar densities as well as the peak of the EUV distribution (EUV mode) collected within the sampling window of each LST_{MSO}-altitude bin (dashed red line). Figure 2b contains the median (solid line) as well as the 25th and 75th percentile values (dashed lines) of the neutral temperature distribution in each bin centered on 200 km altitude. Numbered arrows in each panel indicate local minima (1) and maxima (2 and 3) that are consistent across all species and in the mean of the neutral temperature distribution. Note, however, that these neutral features do not correspond to commensurate minima/maxima in the EUV sampling (dashed red line in Figure 2a) indicating that they are driven by processes other than the inflation of the global thermosphere due to enhanced solar heating. The amplitudes of the features indicated in Figure 2b (blue, red, and black arrows) are, in some cases, similar in magnitude to the spread of the temperature distribution. Nevertheless, the entire distribution of temperatures is seen to shift up and down at the locations of the arrows in Figure 2b, indicating that these are identifiable features in the mean neutral thermosphere. The local minimum indicted by the blue arrow (1) straddles the dusk terminator (dashed vertical line) between 17.5 and 18.5 LST_{MSO}, while the two maxima are observed between 18–19 and 19–20 LST_{MSO}. Another local maximum in $T_{N,200km}$ appears just prior to the terminator at approximately 17.5 LST. However, this predusk feature corresponds to a peak in the local time distribution of EUV sampling and might therefore be a result of the EUV forcing aliasing into the observed local time structure. The variability in Lyman-α irradiance during the time of observation shown in Figure 2 is approximately ±6%. Other observing periods in the morning and evening sectors correspond to Lyman-α variability of up to ±15%. In the following analysis, the data in each bin are filtered to limit the EUV irradiance to ±5% or less.
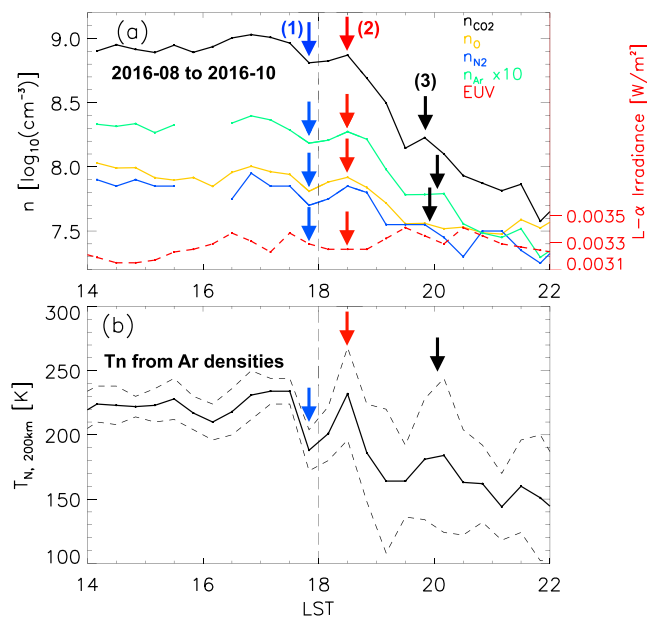
In order to examine whether the thermospheric features highlighted in Figure 2 exhibit interannual and interseasonal stability, additional observational periods are compared corresponding to ±35° latitude MSO in both the evening (Figures 3a and 3b) and morning (Figures 3c and 3d) sectors. It is important to note that the thermospheric temperatures shown in the next two figures are a result of measurements made along a section of the evening and morning regions at an angle which is not entirely parallel to the MSO equator. As such, some latitudinal changes in Thermospheric temperature can be expected to appear even though they are plotted

Figure 2. Binned neutral densities near 180 km (a) from both ascending and descending passes (Ar), descending passes only (CO_2, N_2, and O), and the average measured EUV irradiance for each bin during observations made in 2016. Panel (b) shows the average temperature near 200 km (solid line) along with the 25th and 75th percentile values (dashed lines). The location of nighttime density features (highs and lows) are shown by arrows. Blue arrows (1) indicate density minima between 17.5 and 18.5 LST, red arrows (2) refer to enhancements between 18 and 19 LST, and black arrows (3) to enhancements between 19 and 20 LST, and blue arrows between 21 and 22 LST. EUV = extreme ultraviolet; LST = local solar time.
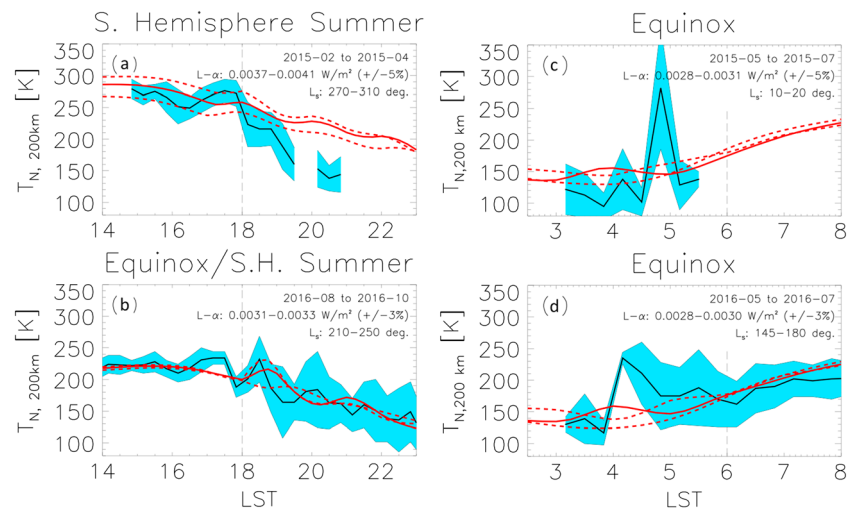
Figure 3. Neutral temperatures in the evening sector between ±35° Mars-Sun-Orbit latitude during 2015 (a) and 2016 (b). Solid lines show the median temperature inside each bin while the blue regions represent the 25th and 75th percentiles in the temperature distribution. The Lyman-α has been filtered to the ranges shown in each panel such that the total variability in irradiance is no more than ±5%. The actual irradiance variability for each of the cases is listed in parentheses in each panel. Red lines indicate Mars Global Ionosphere-Thermosphere Model results as a function of local time at latitudes corresponding to the beginning (dashed line), middle (solid line), and end (dashed line) of the observational period. The panels on the right show results of observations in the morning sector during May to July 2015 (c) and May to July 2017 (d). LST = local solar time.

only as a function of local time. The extent to which these cross sections of the thermosphere vary in latitude is generally 20° or less in the evening region, while the morning cross sections have latitudinal extents of 35° or less. Meanwhile, these same data sets span between 45° and 135° in solar longitude. To estimate the extent to which latitude variability might affect the results, the temperatures from an M-GITM simulation during southern hemisphere summer (Figure 3a) and equinox (Figures 3b–3d) and moderate solar conditions are plotted along with the data. Model temperatures are shown at 200 km altitude and latitudes corresponding to the beginning (dashed red line), middle (solid red line), and end (dashed red line) of each observational period. The model results are not meant to be a direct comparison but only intended to indicate qualitative features and the amount of possible latitudinal variability. The local times and amplitudes of the modeled temperature peaks can change significantly at different latitudes and this needs to be accounted for in any future model-data comparisons.

Temperatures for two independent observational periods of the evening sector are shown in Figure 3. The evening observational periods occur in 2015 and 2016 and correspond to a wide range of EUV conditions (indicated in each panel). The temperatures in Figure 3 are plotted in a manner equivalent to Figure 2b with the solid blue region indicating the short-term variability of the measurements.

Figure 3a shows data collected between February and April 2015 during relatively high solar forcing conditions and Mars solar longitudes (L_s) between 270° and 310° (near perihelion, southern hemisphere summer solstice). A temperature enhancement of approximately 40 K relative to the surrounding temperatures is visible just before 18 LST_{MSO}. A smaller enhancement is also apparent between 18 and 19 LST_{MSO}. The M-GITM model also indicates that two peaks should be visible in this region at a variety of latitudes, though at slightly different local times. Figure 3b corresponds to data collected between August and October 2016 when L_s was between 210° and 250° (near perihelion). Local temperature enhancements of ~40 K are observed within an hour of the dusk terminator. The M-GITM results also indicate a two peak structure but again at different local times.

Note that the local temperature minimum near 18 LST_{MSO} in Figure 3b (2016) is consistent with the location of the decrease in the average altitude profile of CO_2 between 18.3 and 18.6 LST_{MSO} illustrated in Figure 1.

Enhancements in the temperature distributions between 17–18 and 18–19 LST_{MSO} as well as local minima near 18LST_{MSO} are observed during two independent observing periods in the evening sector. In all cases,

the temperature enhancements have a magnitude of 10–40 K above the surrounding temperatures. The location and approximate magnitude of the postdusk enhancement (18–19 LST_{MSO}) is approximately consistent with the equatorial heat island predicted by pre-MAVEN global circulation modeling (Bougher, Pawlowski, et al., 2015) and is similar to the location of heating enhancements manifested in other modeling efforts (Gonzalez-Galindo et al., 2010). The modeled heat island is a thermospheric temperature enhancement spanning low to midlatitudes and local times just after the dusk and just before the dawn terminators. The data presented here are consistent with a low-latitude cross section of such a feature.

Figures 3c and 3d illustrate two observational periods in the morning sector of the Martian thermosphere. Both observing periods correspond to moderate or low solar forcing conditions. Solar forcing and L_s are indicated in each panel. The observing times correspond to equinox in 2015 (c) and equinox in 2016 (d). Predawn and postdawn temperature distributions are low relative to the evening sector and the variability, as represented by the solid blue regions, is relatively high in each bin. Nevertheless, both observing periods indicate the presence of a ~80–100 K temperature enhancement at approximately 4–5 LST_{MSO}. The presence of a temperature peak near the equatorial dawn thermosphere is also consistent with global circulation modeling (Bougher, Pawlowski, et al., 2015, Gonzalez-Galindo et al., 2010), though the exact near-dawn location and magnitude of these features varies from model to model. The M-GITM results plotted in Figures 3c and 3d indicate a model peak that appears at earlier local times and with smaller amplitudes that the observations suggest. The modeled peak is also shown to be sensitive to the latitude of the observation (solid vs. dashed red lines in Figure 3).

5. Discussion

The persistent temperature enhancement at 18–19 hr LST_{MSO} in the equatorial regions is consistent with the postdusk dynamical heating feature discussed by Bougher et al. (1990) and Bougher, Pawlowski, et al., (2015) and is the first direct confirmation that a nighttime density and temperature peak exists in this region. A temperature peak between 4 and 5 local time is also consistent with morning features which are manifested in modeling studies due to dynamical heating and cooling in the presence of converging and diverging neutral winds. Other features such as the predusk enhancement observed consistently at local times between 17 and 18 have no equivalent dynamical heating source suggested by models.

It is possible that some of the observed temperature features are associated at least in part with the presence of a terminator wave. Terminator waves can be generated as the terminator, and the change in solar heating associated with it, passes across the atmosphere of a rotating planet in a way similar to waves generated by the bow of a passing boat. These wave packets have been termed Solar Terminator Waves. In the early 1970s waves of this type at various heights in Earth's atmosphere were theorized (Beer, 1973) and some observations of the ionosphere appeared to confirm their existence (Raitt & Clark, 1973). Accelerometer measurements made by the CHAMP mission provided the first observations of these waves in Earth's thermosphere with amplitudes of 6–8% at 400 km altitude (Forbes et al., 2008; Liu et al., 2009). Forbes and Moudden (2009) used a high-resolution numerical model to show that a terminator wave with neutral density amplitudes of ~20% should exist at Mars at altitudes above 150 km. This modeling description is also consistent with the amplitude of the trough at the dusk terminator as well as the postterminator peak at 18–19 LST_{MSO}.

Detailed model-data comparisons are needed to shed more light on the origin of the observed temperature features. Measurements of thermospheric winds (currently very sparse, Bougher, Roeten, et al., 2017) are also needed to investigate whether the observed density and temperature structures correspond to regions of strong converging winds.

Both the Solar Terminator Waves and dynamical heating enhancement have significant influence on the energy budget of the dusk thermosphere. This should translate to effects felt on neutral-ion and neutral-electron coupling just prior to dusk as well as Jeans escape rates of the warmed neutrals in the postdusk thermosphere.

6. Summary and Conclusions

The MAVEN mission is enabling the detailed study of global thermospheric dynamics at Mars. We have used MAVEN NGIMS data binned in MSO coordinates to analyze the local time structure of the equatorial

thermosphere in the dusk and dawn regions at several seasons and EUV conditions. Results indicate the presence of stationary local time features near the dawn and dusk terminators. In a few of the cases described in this work, nighttime temperature enhancements are shown to have mean temperatures that exceed those in the dayside morning/evening sectors. The results presented here are consistent with the presence of localized dynamical heating feature appearing in global circulation models of the Martian thermosphere. An alternative explanation for the dusk features observed here might also be a terminator wave that is stationary in local time. It is possible that aspects of both phenomena conspire to result in the thermospheric structure observed. Detailed dynamical modeling studies are needed to move forward with the analysis of these dawn and dusk features and the underlying thermal balances near the terminators.

References

Beer, T. (1973). Supersonic generation of atmospheric waves. *Nature*, *242*(5392), 34. https://doi.org/10.1038/242034a0

Bougher, S.W. Bell, J. M., Olsen, K., Roeten, K., Mahaffy, P. R., Elrod, M., et al. (2015). Variability of Mars thermosphere neutral structure from MAVEN Deep Dip observations: NGIMS comparisons with Global Models, AGU Fall 2015, Abst. # P21A-2064.

Bougher, S. W., Brain, D. A., Fox, J. L., Gonzalez-Galindo, F., Simon-Wedlund, C., & Withers, P. G. (2017). Chapter 14: Upper atmosphere and ionosphere. In B. Haberle, M. Smith, T. Clancy, F. Forget, & R. Zurek (Eds.), *The atmosphere and climate of Mars* (pp. 433–463). Cambridge, UK: Cambridge University Press. https://doi.org/10.1017/9781107016187

Bougher, S. W., Jakosky, B., Halekas, J., Grebowsky, J., Luhmann, J., Mahaffy, P., et al. (2015). Early MAVEN Deep Dip campaign reveals thermosphere and ionosphere variability. *Science*, *350*(6261), aad0459. https://doi.org/10.1126/science.aad0459

Bougher, S. W., Pawlowski, D., Bell, J. M., Nelli, S., McDunn, T., Murphy, J. R., et al. (2015). Mars global ionosphere-thermosphere model: Solar cycle, seasonal and diurnal variations of the Mars upper atmosphere. *Journal of Geophysical Research: Planets*, *120*, 311–342. https://doi.org/10.1002/2014JE004715

Bougher, S. W., Roble, R. G., Ridley, E. C., & Dickinson, R. E. (1990). The Mars thermosphere: 2. General circulation with coupled dynamics and composition. *Journal of Geophysical Research*, *95*(B9), 14,811–14,827. https://doi.org/10.1029/JB095iB09p14811

Bougher, S. W., Roeten, K. J., Mahaffy, P. R., Benna, M., Elrod, M. K., Bell, J. M., & Jakosky, B. M. (2017). Variability of the thermospheric temperature and wind structure of Mars: MAVEN NGIMS measurements and corresponding global model simulations, 6th Mars Atmosphere Modeling and Observations Workshop, Granada, Spain, 16–20 January (2017).

England, S. L., Liu, G., Yiğit, E., Mahaffy, P. R., Elrod, M., Benna, M., et al. (2017). MAVEN NGIMS observations of atmospheric gravity waves in the Martian thermosphere. *Journal of Geophysical Research: Space Physics*, *122*, 2310–2335. https://doi.org/10.1002/2016JA023475

Eparvier, F. G., Chamberlin, P. C., Woods, T. N., & Thiemann, E. M. B. (2015). The solar extreme ultraviolet monitor for MAVEN. *Space Science Reviews*, *195*(1–4), 293–301. https://doi.org/10.1007/s11214-015-0195-2

Forbes, J. M., Bruinsma, S. L., Miyoshi, Y., & Fujiwara, H. (2008). A solar terminator wave in thermosphere neutral densities measured by the CHAMP satellite. *Geophysical Research Letters*, *35*, L14802. https://doi.org/10.1029/2008GL034075

Forbes, J. M., & Moudden, Y. (2009). Solar terminator wave in a Mars general circulation model. *Geophysical Research Letters*, *36*, L17201. https://doi.org/10.1029/2009GL039528

Gonzalez-Galindo, F., Bougher, S. W., L'opez-Valverde, M. A., Forget, F., & Murphy, J. (2010). Thermal and wind structure of the Martian thermosphere as given by two general circulation models. *Planetary and Space Science*, *58*(14-15), 1832–1849. https://doi.org/10.1016/j.pss.2010.08.013

Jakosky, B. M., Lin, R. P., Grebowsky, J. M., Luhmann, J. G., Mitchell, D. F., Beutelschies, G., et al. (2015). The Mars atmosphere and volatile evolution (MAVEN) mission. *Space Science Reviews*, *195*(1-4), 3–48. https://doi.org/10.1007/s11214-015-0139-x

Liu, H., Lühr, H., & Watanabe, S. (2009). A solar terminator wave in thermospheric wind and density simultaneously observed by CHAMP. *Geophysical Research Letters*, *36*, L10109. https://doi.org/10.1029/2009GL038165

Mahaffy, P. R., Benna, M., King, T., Harpold, D. N., Arvey, R., Barciniak, M., et al. (2014). The neutral gas and ion mass spectrometer on the Mars atmosphere and volatile evolution mission. *Space Science Reviews*, *195*(1-4), 49–73. https://doi.org/10.1007/s11214-014-0091-1

Nicholson, W. P. (2011). Studies of the Martian upper atmosphere with the UCL Mars thermosphere and ionosphere general circulation model, (Doctoral thesis). UCL (University College London).

Raitt, W. J., & Clark, D. H. (1973). Wave-like disturbances in the ionosphere. *Nature*, *243*(5409), 508–509. https://doi.org/10.1038/243508a0

Ridley, A., Deng, Y., & Tòth, G. (2006). The global ionosphere-thermosphere model. *Journal of Atmospheric and Solar - Terrestrial Physics*, *68*(8), 839–864. https://doi.org/10.1016/j.jastp.2006.01.008

Snowden, D., Yelle, R. V., Cui, J., Wahlund, J. E., Edberg, N. J. T., & Ågren, K. (2013). The thermal structure of titan's upper atmosphere, I: Temperature profiles from Cassini INMS observations. *Icarus*, *226*(1), 552–582. https://doi.org/10.1016/j.icarus.2013.06.006

Zurek, R. W., Tolson, R. A., Bougher, S. W., Lugo, R. A., Baird, D. T., Bell, J. M., & Jakosky, B. M. (2017). Mars thermosphere as seen in MAVEN accelerometer data. *Journal of Geophysical Research: Space Physics*, *122*, 3798–3814. https://doi.org/10.1002/2016JA023641